informa
healthcare

ORIGINAL ARTICLE: RESEARCH

The natural products parthenolide and andrographolide exhibit anti-cancer stem cell activity in multiple myeloma

ELLEN J. GUNN[1], JOHN T. WILLIAMS[1], DANIEL T. HUYNH[2], MICHAEL J. IANNOTTI[1], CHANGHO HAN[3], FRANCIS J. BARRIOS[4], STEPHEN KENDALL[5], CARLOTTA A. GLACKIN[5], DAVID A. COLBY[3,4], & JULIA KIRSHNER[1]

[1]Department of Biological Sciences, [2]School of Pharmacy, [3]Department of Medicinal Chemistry and Molecular Pharmacology, and [4]Department of Chemistry, Purdue University, West Lafayette, IN, USA and [5]Division of Neurosciences, Beckman Research Institute, City of Hope National Medical Center, Duarte, CA, USA

Abstract

Multiple myeloma (MM) is an incurable plasma cell malignancy where nearly all patients succumb to a relapse. The current preclinical models of MM target the plasma cells, constituting the bulk of the tumor, leaving the cancer stem cells to trigger a relapse. Utilizing a three-dimensional tissue culture system where cells were grown in extracellular matrix designed to reconstruct human bone marrow, we tested the anti-multiple myeloma cancer stem cell (MM-CSC) potential of two natural product inhibitors of nuclear factor κB (NFκB). Here we show that parthenolide and andrographolide are potent anti-MM-CSC agents. Both natural products demonstrated preferential toxicity toward MM-CSCs over non-tumorigenic MM cells. Addition of the bone marrow stromal compartment abrogated andrographolide activity while having no effect on parthenolide cytoxicity. This is the first report of a natural product with anti-CSC activity in myeloma, suggesting that it has the potential to improve the survival of patients with MM by eliminating the relapse-causing MM-CSCs.

Keywords: *Myeloma, chemotherapeutic approaches, drug resistance, microenvironment*

Introduction

Multiple myeloma (MM), a cancer arising through the expansion of malignant plasma cells (PCs) in the bone marrow, is an incurable disease displaying heavy resistance to current chemotherapy regimens [1,2]. Patients diagnosed with MM present with hypercalcemia and bone pain due to the presence of lytic bone lesions, renal insufficiency and neuropathy due to the increased levels of monoclonal immuno-globulin, and immunosuppression due to the in-crease in clonal PCs in the bone marrow (BM) [1]. With a low 5-year survival rate, it is estimated that in 2009 there were over 20 000 newly diagnosed cases of MM and over 10 000 deaths within the United States alone. Many factors contribute to the lethal and resilient nature of MM, including spread to multiple bones, occasional presence of extramedul-lary disease, and interaction with hematopoietic microenvironments of the BM that favor MM expansion [3]. Due to the common relapse of MM and low long-term survival, it has been suggested that drug-resistant MM cancer stem cells (MM-CSCs) persist through the course of therapy supported by BM microenvironments [4–8], thus allowing cells to enter a state of proliferative quiescence while remaining resistant to treatment [9].

Cell culture systems in which cells are grown on the surface of tissue culture plastic do not accurately represent normal tissue architecture [10] and the complex interactions between cells and their micro-environment. We have recently described a three-dimensional (3-D) culture system where the extra-cellular matrix and cellular compartments of the BM are reconstructed *in vitro*, recapitulating the native microenvironment of the human BM in which cells

---

Correspondence: Julia Kirshner, Purdue University, Department of Biological Sciences, 201 S. University Street, West Lafayette, IN 47907, USA. Tel: (765)494-2843. Fax: (765)496-1496. E-mail: jkirshne@purdue.edu

occupy distinct niches [9]. In this reconstructed BM (rBM) model, the MM clone undergoes up to 15-fold expansion of the malignant cells. Using the rBM model, we identified MM-CSCs as non-proliferating, drug resistant CD20+ B cells exhibiting multipotent and self-renewal potential. Thus, the rBM model provides a biologically relevant preclinical paradigm enabling the evaluation of therapeutic vulnerabilities of all compartments of the MM clone, including the drug-resistant MM-CSC.

Although the death of malignant cells is a desired characteristic of new anticancer therapies, ridding the tissues of CSCs is essential for preventing a relapse and improving long-term survival. Many of the new anti-cancer therapeutic regimens under development include a component targeting the family of nuclear factor κB (NFκB) transcription factors [11–14]. A recent study demonstrated a negative effect of NFκB inhibitors on tumor stem cell differentiation and proliferation without cytotoxicity toward normal stem and progenitor cells [15]. By utilizing the rBM model, a more accurate evaluation of the efficacy of this family of compounds can be achieved by measuring their potency in the context of the entire MM clone, including MM-CSCs, in an environment closely resembling that of a patient's BM *in vivo*.

Parthenolide (PTH), a naturally occurring sesquiterpene lactone isolated from the feverfew plant (*Tanacetum parthenium*) [16], has been of recent interest since the discovery of its antitumor activity, inhibition of DNA synthesis, and cancer cell proliferation [17–20], and its ability to sensitize cancer cells to other antitumor agents [21–23]. Known to be a powerful inhibitor of NFκB activation, PTH has been observed to induce apoptosis in human acute myelogenous leukemia stem and progenitor cells [15] as well as in MM cell lines [24], without adversely affecting normal hematopoietic cells [15]. This discovery has fueled the efforts to develop PTH as a potential treatment for leukemia [25,26]. Even though PTH represents a novel compound with anti-CSC activity, poor water solubility has limited its direct clinical application. Additionally, a recent phase I clinical study demonstrated that PTH metabolism may further lower its clinical potential [27]. To address the problem of low aqueous solubility, Crooks and co-workers have synthesized aminoparthenolides that have superior solubility [26,28], and preclinical studies so far are promising [25]. The ability of parthenolide to initiate apoptosis in leukemia CSCs was suggested to be a combination of the inhibition of activation of the transcription activity of NFκB and induction of oxidative stress [15,29,30]. As a member of the sesquiterpene lactone class of natural products, parthenolide can bind intracellular thiols, such as glutathione [31], thus initiating oxidative stress through its sequestration. We hypothesized that molecules that inhibit NFκB and also bind glutathione would be cytotoxic to multiple myeloma CSCs and, thus, could be prime candidates for clinical translation.

Andrographolide (AGR), another naturally occurring plant product isolated from *Andrographis paniculata*, is a copalane diterpene that has been investigated less extensively than PTH [32]. Also a known inhibitor of NFκB activation [33], AGR has been shown to bind glutathione [34], and has a history of clinical importance including anti-inflammatory [35], immuno-stimulative [36], and hepatoprotective [37] properties. Recent studies indicate that AGR possesses antitumor activity, stimulating the differentiation of mouse myeloid leukemia cells [38] and inhibiting the growth of human acute promyelocytic leukemia cells [39]. Moreover, AGR contains many polar functional groups which confer higher aqueous solubility compared to PTH, making AGR a promising therapeutic candidate. We have previously shown that melphalan and bortezomib therapies are not curative, because these drugs target CD138+CD56+ MM plasma cells, thus failing to eliminate the CD20+ MM-CSC [9]. Here we show that PTH and AGR are highly effective anti-MM-CSC agents, with AGR displaying increased selectivity for MM-CSCs compared to PTH. The data presented here constitute the first report of natural products with anti-CSC activity in MM.

Materials and methods

Cell lines and patient samples

RPMI-8226 and U266 human multiple myeloma cell lines were purchased from the American Type Culture Collection (ATCC) and cultured per the manufacturer's instructions. After approval from the institutional review boards (Purdue University and University of Alberta) and after informed consent was obtained in accordance with the Declaration of Helsinki, plasma from patients with MM was collected during routine clinic visits at the Cross Cancer Institute, University of Alberta and Horizon Oncology Center, Lafayette, IN.

3-D (rBM) culture

The 3-D tissue culture was set-up as previously described [9]. Briefly, RPMI-8226 or U266 cells were plated at 0.5×10^6 cells/100 μL of rBM matrix (Matrigel/fibronectin, 2:1 vol/vol) in a 48-well plate, and the culture was allowed to gel for 30 min in a 37°C, 5% CO_2 incubator. Subsequently, 1 mL of

growth medium (RPMI-1640 with L-glutamine, 20% fetal bovine serum [FBS], 6.2×10^{-4} M CaCl$_2$, 1×10^{-6} M sodium succinate, 1×10^{-6} M hydrocortisone) was added to each well. To isolate cells from the rBM culture for further analysis, the mixture of cells and matrix was scraped from the culture plates and incubated in 2–3 volumes of ice-cold phosphate buffered saline–ethylenediaminetetraacetic acid (PBS-EDTA) recovery solution (5 mM EDTA, 1 mM NaVO$_4$, 1.5 mM NaF in PBS) for 1 h at 4°C.

To determine the effects of hyaluronic acid (HA) on the drug-resistance of MM cells, plates were coated with 6.25 μg/cm^2 of HA (Sigma) in 1% bovine serum albumin (BSA)/PBS (per the manufacturer's instructions). Subsequently, HA solution was removed, and RPMI-8226 or U266 cells were plated on top of the stromal layer as described above or in the 'MTS assay' section below.

3-D (rBM) co-culture

Human bone marrow stromal cells (FcMSC), a kind gift from Dr. Carlotta Glackin (Beckman Research Institute of the City of Hope National Medical Center), were grown in α-minimum essential medium (α-MEM) (Sigma) supplemented with 20% FBS (Sigma), 1% penicillin/streptomyocin (Sigma), and 1% L-glutamine (Sigma). For co-culture experiments, cells were plated in either 96-well (3×10^4 cells/well) or 48-well (7.5×10^4 cells/well) plates and allowed to adhere overnight. Subsequently, the growth medium was removed, and RPMI-8226 or U266 cells were plated on top of the stromal layer as described for the 'MTS assay' and '3-D (rBM) culture' sections, respectively.

Drug treatments

PTH was purchased from Biomol International and AGR was purchased from Calbiochem. PTH-CF$_3$ and PTH-Cl were prepared as previously described [40]. Drug stocks (45 mM) were stored at -20°C and were prepared by diluting PTH, PTH-CF$_3$, and AGR in ethanol with 10% dimethylsulfoxide (DMSO); PTH-Cl stock was diluted in ethanol with 30% DMSO. Fresh working dilutions of all drugs were made in culture media immediately prior to cell treatment.

Colony forming unit assay

Colony forming unit (CFU) assays were performed as previously described [9]. Cells isolated from rBM cultures were resuspended in 200 μL of Iscove's modified Dulbecco's medium (IMDM) with 2% FBS and mixed with 1 mL Human Methylcellulose Complete Media (R&D Systems) in 35 mm ultra-low binding plates. CFU cultures were incubated for 14 days (or until colonies reached >50 cells) and the resulting colonies were counted.

MTS assay

RPMI-8226 or U266 cells were grown on plastic or in rBM at 1.25×10^5 cells per well in a 96-well plate and treated for 48 h with either 10% DMSO/ethanol vehicle control or various doses of PTH and AGR. The MTS [3-(4,5-dimethylthiazol-2-yl)-5-(3-carboxymethoxyphenyl)-2-(4-sulfophenyl)-2H-tetrazolium] assay was performed using the CellTiter 96 AQ$_{ueous}$ Non-Radioactive Cell Proliferation Assay (MTS) assay kit (Promega) per the manufacturer's instructions. Briefly, 20 μL of combined MTS/phenazine methosulfate (PMS) solution was added to each well and incubated for 90 min in a 37°C, 5% CO$_2$ incubator. The optical density (OD) was subsequently read at 492 nm on a Thermo Multiskan Ascent plate reader.

Flow cytometry

To evaluate the homogeneity of each cell line, cells were stained with CD138–phycoerythrincyanin 5 (PC5) or CD20–phycoerythrin (PE) (Beckman Coulter) for 1 h at room temperature, washed with PBS, and analyzed on a Quanta SC Flow Cytometer (Beckman Coulter). For apoptosis studies, cells were treated with PTH and AGR, isolated from rBM, and stained with annexin V–fluorescein isothiocyanate (FITC) and CD138–PC5 (Beckman Coulter) per the manufacturer's instructions, and 35 000 events were collected and analyzed on a Cell Lab Quanta SC (Beckman Coulter) flow cytometer. Data were analyzed with Cell Lab Quanta Analysis software. For caspase activation studies, cells were treated and isolated from rBM as described above, and activation of caspases 3/7, 8, and 9 detected using the appropriate CaspaTag *In Situ* assay kit (Millipore) per the manufacturer's instructions. Caspase activation was measured on a Quanta SC Flow Cytometer, and the analysis was done using Cell Lab Quanta Analysis software.

Microscopy

Cells isolated from rBM cultures were dried onto microscope slides, fixed with 10% neutral buffered formalin for 15 min at room temperature, and stained with CD138–PC5 (1:100), propidium iodide (PI), and 4′,6-diamidino-2-phenylindole (DAPI) (1:5000) (Beckman Coulter) per the manufacturer's instructions. Slides were imaged on a Zeiss AxioObserver digital microscope and image analysis was done using Zeiss AxioVision software. Differential interference

contrast (DIC) imaging was done directly in rBM culture on a Zeiss AxioObserver digital microscope.

Statistical analysis

Data are presented as the mean $\pm$ SEM of at least three independent experiments performed in triplicate. To calculate LC_{50} (median lethal concentration) values, four-parameter logistic regression was applied to log-transformed percent viability measurements. Significance was analyzed by a two-tail Student's t-test or two-way analysis of variance (ANOVA) and Bonferroni's correction as post-test to compare experiments with multiple parameters. p-Values below 0.05 were considered statistically significant. All analysis was performed using Prism 5.0 software (GraphPad Software).

Results

PTH and AGR are cytotoxic toward MM cells

Under physiological conditions, multiple myeloma cells reside in the BM in contact with the extra-cellular matrix (ECM). The proper ECM micro-environment exerts a protective effect on cancer cells and has been reported to antagonize the effect of drug treatments [41]. Therefore, in order to determine the anti-tumor potential of novel therapeutics, cells have to be grown in the context of their native microenvironment. In this study we utilized the 3-D tissue culture system of rBM, recently designed in our laboratory, to maintain MM cells under physiological conditions [9]. The cell lines used in this study were heterogeneous, and comprised CD138+ and CD20+ cells (Figure 1; results are shown for RPMI-8226 cells; U266 cells had an identical pattern of expression of both CD138 and CD20 antigens). In the rBM system, single cells are plated within the matrix comprising ECM proteins matching the composition of human BM, and after 14 days in rBM culture, MM cell lines, RPMI-8226 and U266, form tumor-like structures which resemble those seen after culturing primary bone marrow cells from patients with MM in this system [9,42].

PTH, a natural product isolated from the feverfew plant, has recently been shown to be cytotoxic toward MM cells in conventional tissue
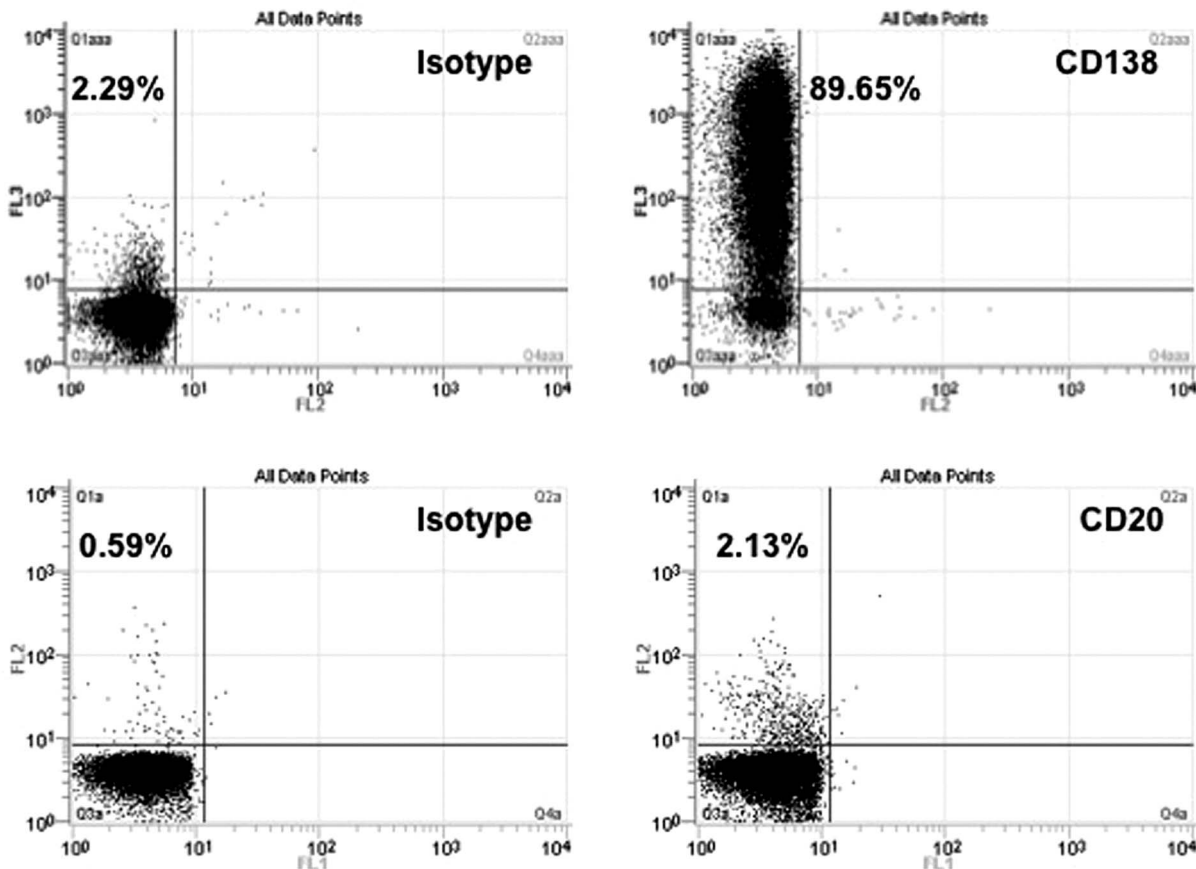

Figure 1. A sub-population of CD20+ B lymphocytes is present in the RPMI-8226 cell line. RPMI-8226 cells were stained with CD138–PC5 or CD20–PE and the presence of the plasma and B cell populations was evaluated by flow cytometry.

cultures [Figure 2(A)] [24]. However, standard culture systems (2-D) where cells are grown in suspension or attached to the plastic surface of a tissue culture flask fail to take into account the adhesion-mediated drug resistance conferred by the ECM. Therefore, we sought to determine whether the anti-myeloma activity of PTH could overcome drug resistance mediated by the interaction of cells with the surrounding ECM. Based on LC$_{50}$ values determined for 2-D and rBM cultures, cells cultured using conventional methods were 1.5–1.6 times more sensitive to PTH than cells cultured in rBM [Figures 3(A) and 3(C), Table I]. Since inhibition of NFκB activation is likely the main mechanism of parthenolide toxicity [43], we tested the anti-myeloma potential of AGR, another natural product inhibitor of NFκB activation isolated from the *Andrographis* plant. Similar to the results obtained with PTH, cells grown in 2-D cultures were more sensitive to AGR than cells grown in rBM [Figures 3(B) and 3(D)]. In both 2-D and rBM cultures PTH was more cytotoxic than AGR, but both drugs had significant anti-myeloma activity [Figures 3(A)–3(D) and 4].

BM stroma has been implicated in conferring resistance to multiple chemotherapeutic agents. Therefore, we tested the response of MM cells to PTH and AGR in co-culture with BM stromal cells in both 2-D and rBM cultures. Addition of stromal

cells to the PTH treated cultures did not affect the efficacy of the drug. However, the response of MM cells to AGR was completely abrogated in both 3-D and rBM co-cultures [Figures 3(A)–3(D), Table I]. These results suggest that PTH and AGR induce cytotoxicity through different mechanisms. An additional component of the BM ECM, HA, is expressed at high levels in BM, and was absent from the matrix mixture of the rBM culture. Thus, we tested the response of MM cells grown on HA coated plates to PTH and AGR. The addition of HA had no affect on cytotoxicity of either PTH or AGR [Figures 3(C) and 3(D), Table I]. Therefore, we conclude that while HA may be an important suvival and proliferation factor in MM, adhesion to HA does not induce resistance to PTH and AGR.

PTH and AGR exhibit anti-myeloma CSC activity

The nearly 100% rate of relapse of patients with MM implies that none of the current therapies are capable of completely eliminating all neoplastic cells from the patients' BM, allowing for the remaining tumor-initiating cells to re-initiate the myeloma lesions. This failure of multiple agents and their combinations to cure MM emphasizes the need for new therapeutic regimens which, in addition to targeting the non-tumorigenic cells constituting the bulk of the tumor and lacking tumor-initiation capacity, will target the tumor-initiating CSCs. We and others have previously described the resistance of CSCs in MM to multiple conventional chemotherapeutic agents [9,44,45]. The recent success of using PTH as an anti-CSC agent in acute myelogenous leukemia [15] prompted us to test the anti-MM-CSC activity of PTH and AGR in the context of adhesion-mediated drug resistance. MM cells treated with either PTH or AGR were isolated from rBM cultures 48 h post-treatment and re-plated into methylcellulose-based CFU assays. CFU assays are specially formulated to allow colony formation by stem cells, but not by other cells, and MM-CSCs have been shown to self-renew and form colonies in CFU media [9,44]. Unlike the use of surface markers, which are unreliable in isolating stem cells from many cancers, the CFU assay allows a functional readout of the frequency and viability of CSCs from hematological malignancies. After 14 days in CFU culture, the frequency of MM-CSCs remaining after PTH and AGR treatment was assessed by counting the colonies of >50 cells visible in each plate. The viability of MM-CSCs was then presented as a percentage of colonies observed in the PTH and AGR treated samples compared to the vehicle treated controls. Both PTH and AGR induced cell death in MM-CSCs in a dose-dependent manner [Figures 3(E)
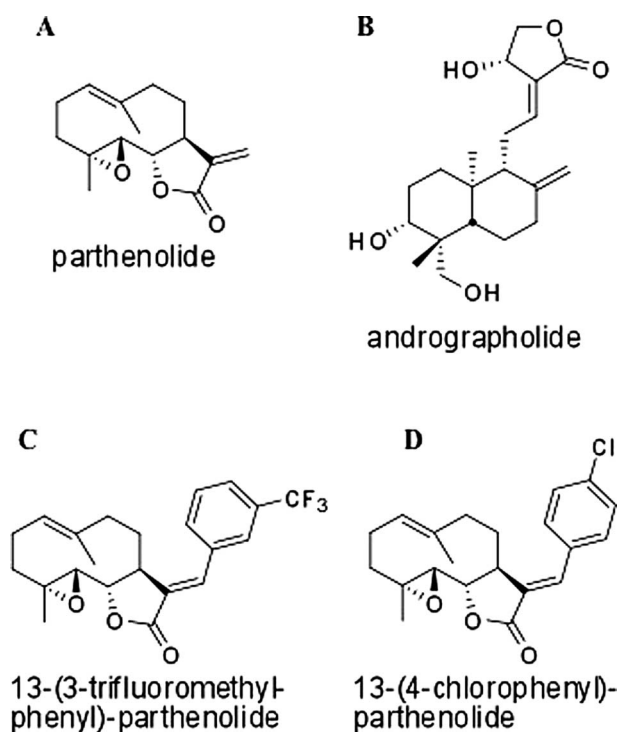

Figure 2. Structures of PTH, AGR, and related derivatives. (A) Parthenolide; (B) andrographolide; (C) 13-(3-trifluoromethylphenyl)-parthenolide; (D) 13-(4-chlorophenyl)-parthenolide.
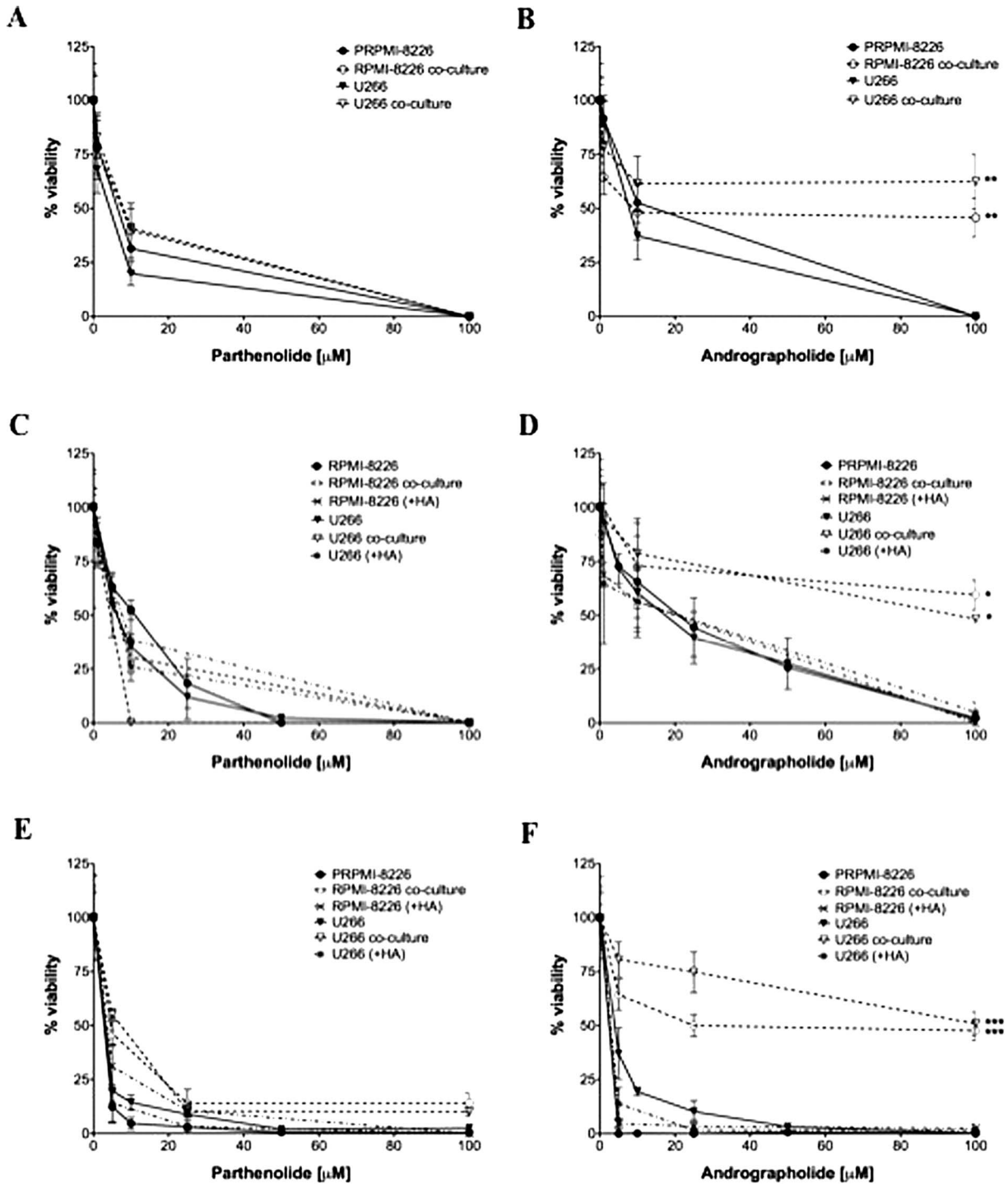
Figure 3. Multiple myeloma tumor and CSCs are sensitive to PTH and AGR. (A, B) RPMI-8226 and U266 cells were grown in 2-D cultures alone or in co-culture with BM stromal cells and treated with PTH (A) or AGR (B) for 48 h. Cell viability was assessed by MTS assay. All values were normalized to cell viability of vehicle treated controls ($n = 3$ independent experiments performed in triplicate). (C, D) RPMI-8226 and U266 cells were grown in rBM cultures alone or in co-culture with BM stromal cells, or in HA coated plates, and treated with PTH (C) or AGR (D) for 48 h. Cells were isolated from rBM and viability was measured by MTS assay. All measurements were normalized to cell viability of vehicle treated controls ($n = 4$ independent experiments performed in triplicate). (E, F) RPMI-8226 and U266 cells were grown in rBM cultures alone or in co-culture with BM stromal cells, or in HA coated plates, and treated with PTH (E) or AGR (F) for 48 h. Cells were isolated from rBM cultures and plated into a methylcellulose-based CFU assay. MM-CSC viability was assessed after 14 days in CFU culture by counting the number of colonies present after each treatment. All colony counts were normalized to those of vehicle treated controls ($n = 4$ independent experiments performed in triplicate). Difference between culture conditions was analyzed by ANOVA ($^*p < 0.05$, $^{**}p < 0.01$, $^{***}p < 0.001$).

and 3(F)]. Interestingly, both drugs exhibited higher toxicity toward MM-CSCs ($LC_{50} = 1.5–3.5$ μM) compared to toxicity toward non-CSCs ($LC_{50} = 7–15$ μM) (Table I). The difference in sensitivity to PTH and AGR between the two cell lines is due to the differences in frequency of CSCs in RPMI-8226 and U266 lines at 2.62% and 1.86%, respectively. The selectivity ratio (the ratio of LC_{50} values) of PTH and AGR for tumorigenic MM-CSCs compared to the entire population constituting the bulk of the tumor in RPMI-8226 cells was 6.3 and 10, respectively (Table I). The selectivity ratio of PTH and AGR in U266 was 3 and 4.4, respectively. The nearly two-fold higher selectivity of AGR for MM-CSCs compared with PTH is quite striking, since PTH selectivity for leukemic CSCs was one of the critical factors for its rapid translation into the clinic [15].

We also tested the effects of BM stromal cells and HA on the anti-MM-CSC activity of PTH and AGR. RPMI-8226 and U266 cells grown on HA coated plates exhibited the same response to PTH and AGR as those grown in rBM cultures, with LC_{50} values for the MM-CSC cytotoxicity of 2.4 μM and 3 μM for PTH and AGR, respectively [Figures 3(E) and 3(F), Table I]. The addition of BM stromal cells to the rBM cultures treated with PTH also did not affect the efficacy of the drug, while the anti-MM-CSC response of both cell lines to AGR was completely abrogated in BM stromal co-cultures [Figures 3(E) and 3(F)].

Structural changes to PTH affect its anti-tumor activity

PTH has been shown to preferentially target CSCs in leukemia without toxicity toward normal hematopoietic stem cells [15], and in our assays showed high specificity for MM-CSCs over non-tumorigenic cells constituting the bulk of the tumor (Table I). The activity of PTH against CSCs in leukemia provided a strong impetus for making structural derivatives with increased water solubility [26,28,40]. One such derivative, 13-(3-trifluoro-methylphenyl)-parthenolide ($PTH-CF_3$), emerged as an active fluorinated analog [40]. Fluorinated compounds have significant potential to serve as metabolic and biological probes and imaging agents for positron emission tomography (PET). Therefore, we sought to determine the potential of $PTH-CF_3$ as a biological probe in MM by verifying its activity in this disease. In order to further explore structure–activity relationships of PTH, we examined another structural analog, 13-(4-chlorophenyl)-parthenolide (PTH-Cl). Under physiological conditions provided by the rBM model, $PTH-CF_3$ exhibited dose-dependent anti-MM activity, with greater cytotoxicity toward MM-CSCs than non-tumorigenic cells [Figure 5]. On the other hand, PTH-Cl had higher

Table I. LC_{50} values for anti-tumor and anti-CSC activity of PTH, $PTH-CF_3$, PTH-Cl, and AGR*.

Cells	Culture		PTH	$PTH-CF_3$	PTH-Cl	AGR
RPMI-8226	2-D	None	6.5	ND	ND	10
		Stroma	5	ND	ND	NR
	3-D	rBM	10	60	25	15
		rBM w/ stroma	7	ND	ND	NR
		HA	6	ND	ND	13
	CFU	rBM	1.6	13.5	60	1.5
		rBM w/ stroma	4.8	ND	ND	NR
		HA	2	ND	ND	2.3
		Ratio[†]	6.3	4.4	0.42	10
U266	2-D	None	4.3	ND	ND	8
		Stroma	7	ND	ND	NR
	3-D	rBM	7	57.5	22	15.3
		rBM w/ stroma	6	ND	ND	NR
		HA	7.3	ND	ND	12
	CFU	rBM	2.3	25	50	3.5
		rBM w/ stroma	5.5	ND	ND	NR
		HA	2.4	ND	ND	3
		Ratio[†]	3	2.3	0.44	4.4

*LC_{50} values are presented in μM.

[†]Ratios represent preferential selectivity of each drug for the MM-CSCs [sensitivity ratio = LC_{50}(3-D, rBM)/LC_{50}(CFU, rBM), i.e. LC_{50}(total cells in rBM)/LC_{50}(MM-CSCs treated in rBM and transferred to CFU for MM-CSC evaluation)].

LC_{50}, median lethal concentration; CSC, cancer stem cell; PTH, parthenolide; AGR, andrographolide; 2-D, two-dimensional; CFU, colony forming unit; rBM, reconstructed bone marrow; w/, with; HA, hyaluronic acid; ND, not determined; NR, LC_{50} not reached, MM-CSCs, multiple myeloma cancer stem cells.
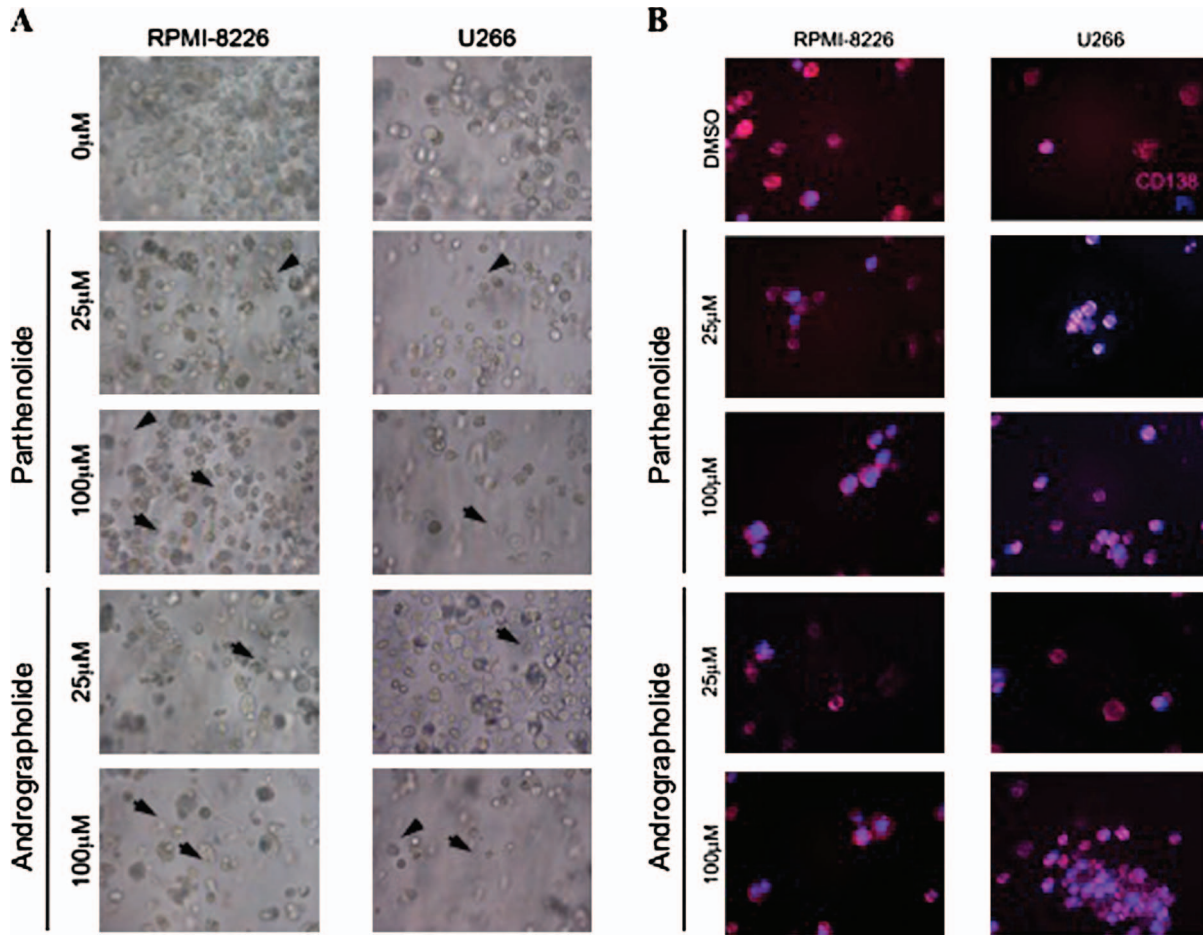
Figure 4. PTH and AGR are cytotoxic in rBM culture. (A) RPMI-8226 and U266 cells were grown in rBM cultures and treated with PTH or AGR for 48 h. DIC imaging was done directly in rBM culture (arrowheads mark dying cells; magnification $\times 10$). (B) Cells were grown as in (A), isolated from the rBM, and stained with CD138 (red) and propidium iodide (blue) (magnification $\times 10$).
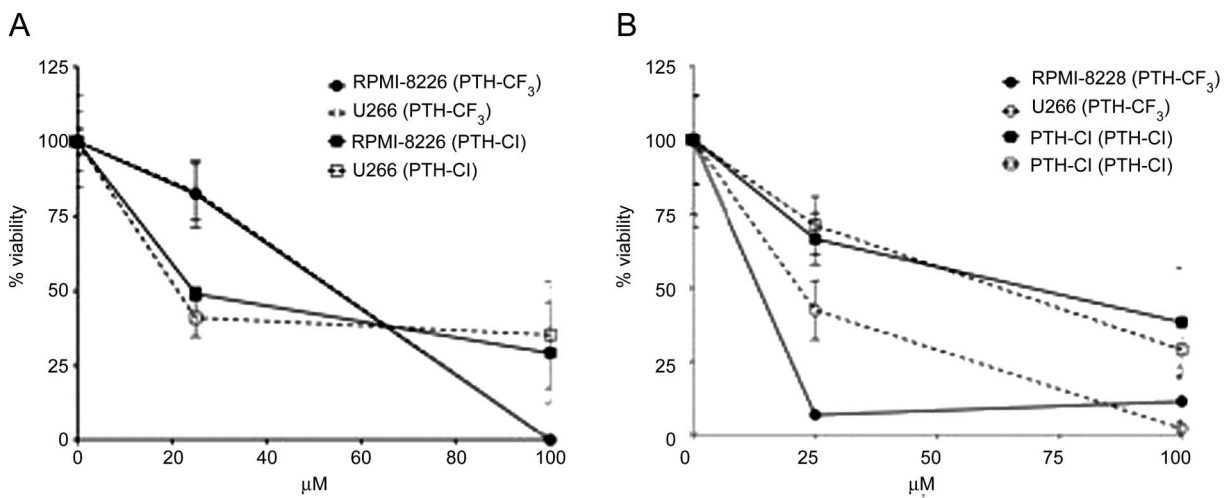

Figure 5. Multiple myeloma tumor and CSCs are less sensitive to structural derivatives of PTH than to the parent compound. (A) RPMI-8226 and U266 cells were grown in rBM cultures and treated with PTH-CF$_3$ or PTH-Cl for 48 h. Cells were isolated from the rBM and the viability was measured by MTS assay. All measurements were normalized to cell viability of vehicle treated controls ($n = 4$ independent experiments performed in triplicate). (B) Cells were grown and treated as in (A), isolated from the rBM cultures, and plated into a methylcellulose-based CFU assay. MM-CSC viability was assessed after 14 days in CFU culture by counting the number of colonies present after each treatment. All cell counts were normalized to those of vehicle treated controls ($n = 4$ independent experiments performed in triplicate).

cytotoxicity toward non-tumorigenic cells than MM-CSCs [Figure 5]. The selectivity ratios of PTH-CF$_3$ and PTH-Cl for MM-CSCs over the non-tumorigenic population in RPMI-8226 cells were 4.4 and 0.42, respectively, and for U266 cells the selectivity ratios were 2.3 and 0.44 (Table I). In striking contrast to PTH and PTH-CF$_3$, both of which were more selective toward CSCs than the non-tumorigenic counterparts, PTH-Cl exhibited a complete loss of selectivity for the MM-CSCs. This comparison not only highlights the critical need to examine potential therapeutic compounds in more robust assays, rather than in traditional 2-D cultures, but also illustrates the importance of understanding the structure–activity relationships of emerging therapeutics for selectivity toward CSCs.

PTH and AGR induce caspase-mediated apoptosis in MM cells

PTH and AGR are thought to induce cell death by blocking activation of NFκB. Since NFκB is responsible for transcription of a number of inhibitors of apoptosis, it is logical that blocking NFκB will lead to cell death in the affected cells. Cell death can occur by either of two mechanisms: apoptosis, programmed cell death; or necrosis, non-specific cell death. The preferential selectivity of PTH and AGR toward CSCs suggests that these compounds eliminated their target cells by inducing apoptosis. Although plasma membrane integrity is disrupted during both apoptosis and necrosis, making cells permeable to dyes such as PI, an early apoptotic event is the translocation of phosphatidylserine from the inside leaflet of the plasma membrane to the outside. This translocation can be detected by the binding of annexin V to the externalized phosphatidylserine. Apoptotic cell death was induced in both CD138+ plasma cells and CD138− cells in response to PTH and AGR treatment. Cells in the early stages of apoptosis were positive for annexin V alone, and those in the late stages of apoptosis were positive for both annexin V and PI [Figure 6(A)]. We and others have demonstrated that CD20+ B cells consistute the CSC population in MM [9,44]; therefore, the CD138− fraction of RPMI-8226 and U266 cells is enriched for MM-CSCs. As described above, MM-CSCs are more sensitive to PTH and AGR than are their non-tumorigenic counterparts, and after treatment with PTG and AGR a higher percentage of annexin V positive cells was observed in the CD138− (76.8% and 75.32% for PTH and AGR, respectively) than in the CD138+ population (44.6% and 40.6% for PTH and AGR, respectively) [Figure 6(B)].

Caspases, a family of cysteine proteases, initiate a cascade of proteolytic cleavages resulting in cell death. Initiator caspases 8 and 9 are responsible for initiation of the apoptotic cascade by activating the effector caspases 3 and 7, which in turn cleave numerous cellular protein substrates and mediate the final stages of apoptotic cell death. Treatment with PTH or AGR activated caspases 8, 9, and 3/7 in both RPMI-8226 and U266 cells (Figure 7). The major caspases activated in the RPMI-8226 cells by PTH or AGR were caspases 8 and 3/7 [Figures 7(A) and 7(C)]. However, treatment of U266 cells with PTH and AGR activated caspases 8 and 9 to the same degree [Figures 7(B) and 7(D)]. Therefore, we conclude that while PTH and AGR activate an apoptotic response in MM cells, the specific mechanism of cell death is likely cell-dependent.

Discussion

MM remains incurable even with the recent development of highly effective and potent therapies such as bortezomib and lenalidomide. The inability of the new therapeutic modalities to eliminate the tumor and prevent a relapse, which is nearly 100% in MM, suggests the presence of a drug-resistant malignant cell population capable of initiating the growth of new tumors. CSCs have been isolated from both hematopoietic and solid malignancies and are characterized as rare drug-resistant cells with tumorigenic capacity, while the bulk of the tumor mass comprises highly proliferative cells lacking the ability to initiate new malignant growth. Our previous study demonstrated that while bortezomib is highly potent against clonotypic plasma cells from patients with myeloma, its selectivity for these cells makes bortezomib an ineffective therapy against MM-CSCs that exhibit a B cell phenotype [9,44]. Therefore, new treatment strategies have to be developed to specifically target MM-CSCs, taking into account the effects of both ECM and stroma. In the study presented here we describe the anti-CSC activity of PTH and AGR, active ingredients in medicinal plants feverfew and *Andrographis paniculata* used in traditional medicine as anti-inflammatory agents with fever reducing properties. Both PTH and AGR efficiently targeted MM-CSCs with LC$_{50}$ values ranging from 1.6 to 3.5 μM. MM-CSCs were selectively targeted by both PTH and AGR, with higher selectivity ratios for CSCs than non-tumorigenic tumor mass, as measured by the ratio of LC$_{50}$ values between MM-CSC viability after treatment with PTH or AGR, as assessed in CFU assays, and total cell viability after treatment in rBM culture. U266 cells were slightly less responsive to PTH and AGR than RPMI-8226 cells, possibly due to their ability to
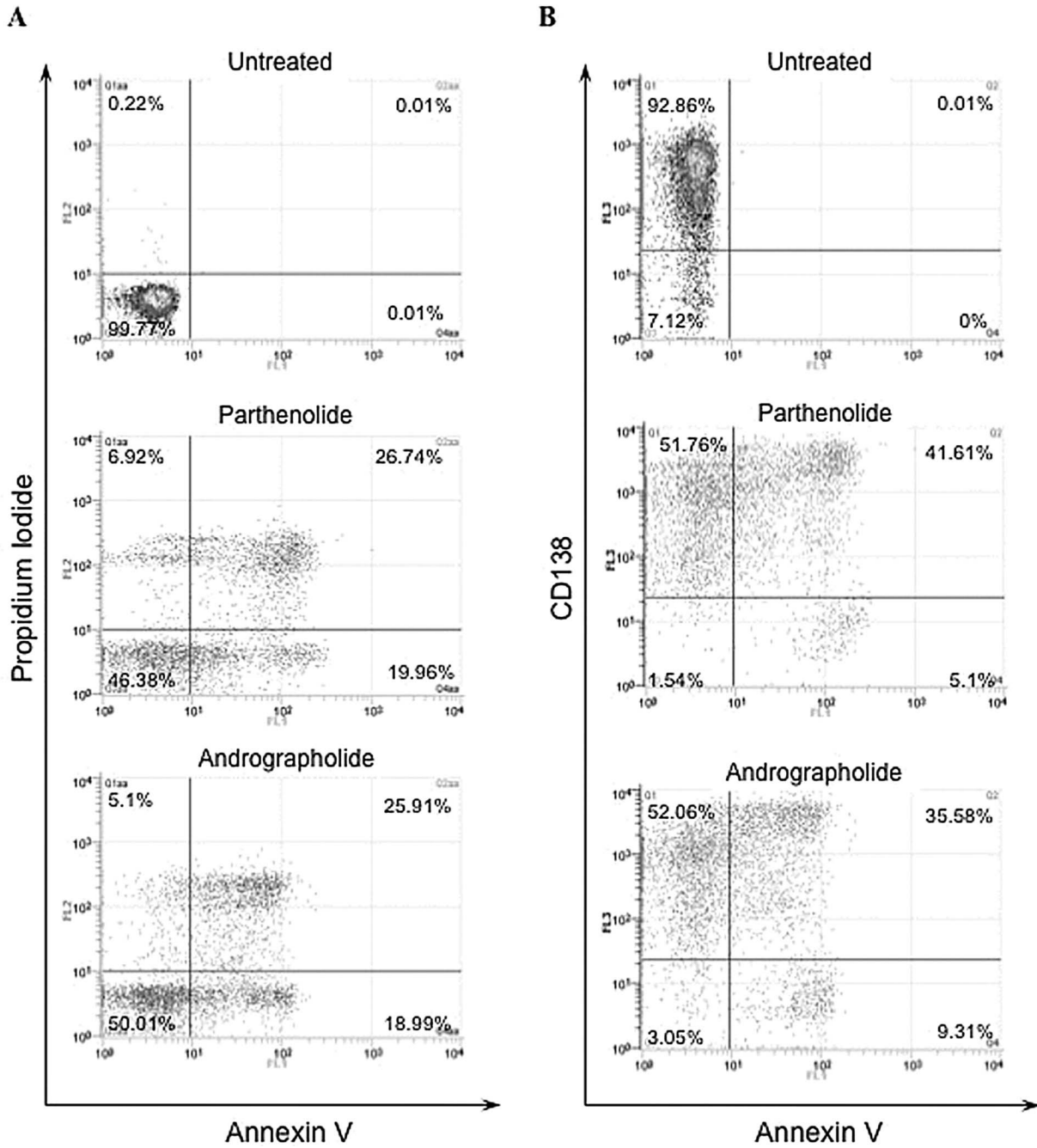
Figure 6. PTH and AGR induce apoptosis in multiple myeloma cells. RPMI-8226 and U266 cells were grown in rBM cultures and treated with 25 μM of PTH or AGR for 18 h. Cells were isolated from the rBM and triple stained with CD138–PC5, annexin V–FITC, and propidium iodide. (A) A density plot of propidium iodide exclusion versus annexin V expression; (B) a density plot of CD138 expression versus annexin V.

secrete interleukin-6 (IL-6), which in rBM cultures without the stromal component acts in an autocrine fashion to promote cell growth and survival [46]. In contrast, RPMI-8226 cells do not secrete IL-6, and thus were more responsive to PTH and AGR. Although the LC_{50} value of PTH and AGR was higher for U266 cells, the efficient targeting of the MM-CSC subpopulation in this cell line suggests

that both PTH and AGR can overcome the protective effects of IL-6. Additionally, the presence of IL-6 in U266, but not RPMI-8226, cultures could explain the observed differences in caspase 9 activation between these cell lines.

Interestingly, AGR was nearly two-fold more selective for MM-CSCs than PTH. This preferential selectivity of AGR is a key discovery, and strongly
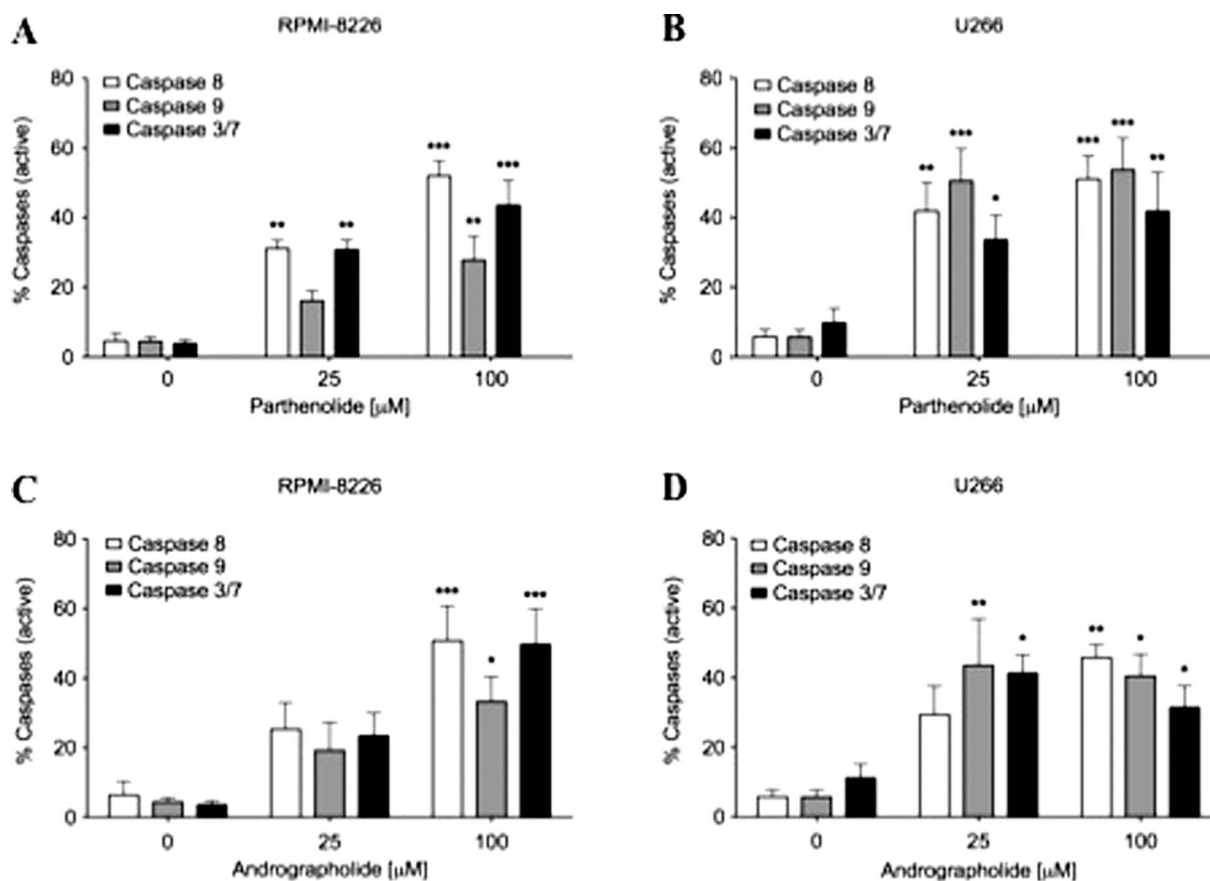
Figure 7. PTH and AGR induce apoptosis of multiple myeloma cells through the activation of caspases. MM cell lines were grown in rBM cultures and treated with PTH or AGR for 48 h. After treatment, cells were isolated from rBM and assayed for the presence of active initiator caspases 8, 9, and effector caspases 3/7. Caspase activity was measured by flow cytometry using caspase-specific fluorochrome inhibitor of caspase (FLICA) apoptosis detection kits ($n = 3$ independent experiments performed in triplicate). (A) RPMI-8226 cells treated with parthenolide; (B) U266 cells treated with parthenolide; (C) RPMI-8226 cells treated with andrographolide; (D) U266 cells treated with andrographolide. Caspase activation at different drug doses as compared to vehicle treated controls (0 µM) (*$p < 0.05$, **$p < 0.01$, ***$p < 0.001$).

supports the need for additional translational studies of AGR in MM. Indeed, the specificity of PTH for myelogenous leukemia stem cells [15] fueled the subsequent translational efforts [25], and concomitantly catalyzed the search for new compounds with selectivity for CSCs [47]. However, loss of AGR-mediated cytotoxicity in BM stromal co-cultures emphasizes the complexity of the system, and stresses the need to evaluate potential therapeutic agents under physiological conditions.

Natural products continue to be a tremendous source of compounds for drug discovery, especially in cancer. After the discovery of the specificity of PTH for leukemia CSCs [15], PTH derivatives with enhanced water solubility were developed [26,28]. Even though solubility was one of the pharmacologically limiting factors of PTH, its metabolism is another concern [26,27]. We prepared a fluorinated PTH derivative (PTH-CF$_3$) as a potential probe [40] to identify metabolites of PTH, and demonstrated

that, similar to the parent compound, PTH-CF$_3$ retained selectivity for MM-CSCs. These findings are contrasted by PTH-Cl, which demonstrates how subtle structural changes eliminate the CSC selectivity.

The work presented here highlights the mostly unexplored aspects of preclinical testing: evaluating the efficacy of therapeutic agents in the context of cell–cell and cell–ECM adhesion-mediated drug resistance, and evaluating the efficacy of novel therapeutics against CSCs. Our previous studies and the work of others have pointed toward CD20+ lymphocytes as the CSCs in MM [9,44]. However, the failure of rituximab as a MM therapeutic has raised questions regarding the identity of MM-CSCs. The data demonstrating the inefficiency of rituximab to treat MM can be explained by a number of factors. The efficacy of rituximab is dependent on the high level of expression of CD20 on the cell surface. Based on our analysis and that of

Matsui and colleagues, MM cells are weakly positive for CD20, and constitute a minor population of malignant cells in patients with MM and cell lines. Thus, it is possible that there are not enough CD20 molecules on the surface of MM cells for rituximab to be effective. Additionally, since CD20+ cells constitute only a minor population of MM cells, the regimen of rituximab administration will likely be crucial to the success of this therapy. If administered at the wrong time during disease progression, targeting of rituximab to the MM-CSCs may be hindered, thus further lowering its efficacy. The large volume of evidence that has accumulated in support of the CD20 phenotype of the MM-CSC suggests that rituximab should be evaluated as an anti-MM-CSC agent in combination with conventional chemotherapies which eliminate the bulk of the tumor.

The comprehensive reconstruction of the BM microenvironment in rBM cultures allows expanded monitoring of drug impact on both tumorigenic and non-tumorigenic tumor populations under physiological conditions. MM cells become resistant to conventional chemotherapeutic agents when cultured in contact with ECM [48–50]. In our study, MM cells grown in contact with ECM in 3-D cultures were nearly twice less sensitive to PTH and AGR as the same cells cultured under standard conditions. Therefore, to ensure that the observed toxicity of PTH and AGR against MM-CSCs takes into account adhesion-mediated drug resistance, we treated the cells in the rBM, and then transferred the surviving cells to the CFU assay to assess the frequency of the surviving MM-CSCs. As discussed above, we determined that PTH and AGR are highly selective for MM-CSCs compared to the non-tumorigenic populations. Additionally, it has been previously shown that PTH does not target normal hematopoietic stem cells [15], thus further raising the value of this compound as a potential anti-tumor therapeutic. The rBM is the only available model within which the drug-resistant properties of MM can be assessed in culture, and therapies targeted against MM-CSCs can be readily tested. The selective toxicity of AGR in MM-CSCs is a novel result, and although synthetic derivatives of AGR have been prepared as potential anticancer agents [32], the structure–activity relationships remain unexplored. The selectivity of AGR for MM-CSCs provides a strong impetus for further translational efforts.

Acknowledgements

References

1. Bataille R, Manolagas SC, Berenson JR. Pathogenesis and management of bone lesions in multiple myeloma. Hematol Oncol Clin North Am 1997;11:349–361.
2. Greipp PR, San Miguel J, Durie BG, et al. International staging system for multiple myeloma. J Clin Oncol 2005;23:3412–3420.
3. Caligaris-Cappio F, Bergui L, Gregoretti MG, et al. Role of bone marrow stromal cells in the growth of human multiple myeloma. Blood 1991;77:2688–2693.
4. Donnenberg VS, Donnenberg AD. Multiple drug resistance in cancer revisited: the cancer stem cell hypothesis. J Clin Pharmacol 2005;45:872–877.
5. Pilarski LM, Hipperson G, Seeberger K, Pruski E, Coupland RW, Belch AR. Myeloma progenitors in the blood of patients with aggressive or minimal disease: engraftment and self-renewal of primary human myeloma in the bone marrow of NOD SCID mice. Blood 2000;95:1056–1065.
6. Pilarski LM, Seeberger K, Coupland RW, et al. Leukemic B cells clonally identical to myeloma plasma cells are myeloma-genic in NOD/SCID mice. Exp Hematol 2002;30:221–228.
7. Reiman T, Seeberger K, Taylor BJ, et al. Persistent preswitch clonotypic myeloma cells correlate with decreased survival: evidence for isotype switching within the myeloma clone. Blood 2001;98:2791–2799.
8. Pilarski LM, Baigorri E, Mant MJ, et al. Multiple myeloma includes phenotypically defined subsets of clonotypic CD20+ B cells that persist during treatment with rituximab. Clin Med Oncol 2008;2:275–287.
9. Kirshner J, Thulien KJ, Martin LD, et al. A unique three-dimensional model for evaluating the impact of therapy on multiple myeloma. Blood 2008;112:2935–2945.
10. Barcellos-Hoff MH, Aggeler J, Ram TG, Bissell MJ. Functional differentiation and alveolar morphogenesis of primary mammary cultures on reconstituted basement membrane. Development 1989;105:223–235.
11. Feinman R, Koury J, Thames M, Barlogie B, Epstein J, Siegel DS. Role of NF-kappaB in the rescue of multiple myeloma cells from glucocorticoid-induced apoptosis by bcl-2. Blood 1999;93:3044–3052.
12. Giuliani N, Colla S, Rizzoli V. New insight in the mechanism of osteoclast activation and formation in multiple myeloma: focus on the receptor activator of NF-kappaB ligand (RANKL). Exp Hematol 2004;32:685–691.
13. Karin M. Nuclear factor-kappaB in cancer development and progression. Nature 2006;441:431–436.
14. Mitsiades CS, Mitsiades NS, Munshi NC, Richardson PG, Anderson KC. The role of the bone microenvironment in the pathophysiology and therapeutic management of multiple myeloma: interplay of growth factors, their receptors and stromal interactions. Eur J Cancer 2006;42:1564–1573.
15. Guzman ML, Rossi RM, Karnischky L, et al. The sesquiterpene lactone parthenolide induces apoptosis of human acute myelogenous leukemia stem and progenitor cells. Blood 2005;105:4163–4169.
16. Knight DW. Feverfew: chemistry and biological activity. Nat Prod Rep 1995;12:271–276.

17. Ross JJ, Arnason JT, Birnboim HC. Low concentrations of the feverfew component parthenolide inhibit in vitro growth of tumor lines in a cytostatic fashion. Planta Med 1999;65:126–129.

18. Wiedhopf RM, Young M, Bianchi E, Cole JR. Tumor inhibitory agent from Magnolia grandiflora (Magnoliaceae). I. Parthenolide. J Pharm Sci 1973;62:345.

19. Woynarowski JM, Konopa J. Inhibition of DNA biosynthesis in HeLa cells by cytotoxic and antitumor sesquiterpene lactones. Mol Pharmacol 1981;19:97–102.

20. Zhang S, Ong CN, Shen HM. Critical roles of intracellular thiols and calcium in parthenolide-induced apoptosis in human colorectal cancer cells. Cancer Lett 2004;208:143–153.

21. Nakshatri H, Rice SE, Bhat-Nakshatri P. Antitumor agent parthenolide reverses resistance of breast cancer cells to tumor necrosis factor-related apoptosis-inducing ligand through sustained activation of c-Jun N-terminal kinase. Oncogene 2004;23:7330–7344.

22. deGraffenried LA, Chandrasekar B, Friedrichs WE, et al. NF-kappa B inhibition markedly enhances sensitivity of resistant breast cancer tumor cells to tamoxifen. Ann Oncol 2004;15:885–890.

23. Karin M, Yamamoto Y, Wang QM. The IKK NF-kappa B system: a treasure trove for drug development. Nat Rev Drug Discov 2004;3:17–26.

24. Suvannasankha A, Crean CD, Shanmugam R, et al. Anti-myeloma effects of a sesquiterpene lactone parthenolide. Clin Cancer Res 2008;14:1814–1822.

25. Guzman ML, Rossi RM, Neelakantan S, et al. An orally bioavailable parthenolide analog selectively eradicates acute myelogenous leukemia stem and progenitor cells. Blood 2007;110:4427–4435.

26. Neelakantan S, Nasim S, Guzman ML, Jordan CT, Crooks PA. Aminoparthenolides as novel anti-leukemic agents: discovery of the NF-kappaB inhibitor, DMAPT (LC-1). Bioorg Med Chem Lett 2009;19:4346–4349.

27. Curry EA 3rd, Murry DJ, Yoder C, et al. Phase I dose escalation trial of feverfew with standardized doses of parthenolide in patients with cancer. Invest New Drugs 2004; 22:299–305.

28. Nasim S, Crooks PA. Antileukemic activity of aminoparthenolide analogs. Bioorg Med Chem Lett 2008;18:3870–3873.

29. Hassane DC, Guzman ML, Corbett C, et al. Discovery of agents that eradicate leukemia stem cells using an in silico screen of public gene expression data. Blood 2008;111:5654–5662.

30. Steele AJ, Jones DT, Ganeshaguru K, et al. The sesquiterpene lactone parthenolide induces selective apoptosis of B-chronic lymphocytic leukemia cells in vitro. Leukemia 2006;20:1073–1079.

31. Schmidt TJ. Helenanolide-type sesquiterpene lactones–III. Rates and stereochemistry in the reaction of helenalin and related helenanolides with sulfhydryl containing biomolecules. Bioorg Med Chem 1997;5(4) 107: 645–653.

32. Nanduri S, Nyavanandi VK, Thunuguntla SS, et al. Synthesis and structure-activity relationships of andrographolide analogues as novel cytotoxic agents. Bioorg Med Chem Lett 2004;14:4711–4717.

33. Hidalgo MA, Romero A, Figueroa J, et al. Andrographolide interferes with binding of nuclear factor-kappaB to DNA in HL-60-derived neutrophilic cells. Br J Pharmacol 2005;144:680–686.

34. Zhang Z, Chan GK, Li J, Fong WF, Cheung HY. Molecular interaction between andrographolide and glutathione follows second order kinetics. Chem Pharm Bull (Tokyo) 2008;56:1229–1233.

35. Xia YF, Ye BQ, Li YD, et al. Andrographolide attenuates inflammation by inhibition of NF-kappa B activation through covalent modification of reduced cysteine 62 of p50. J Immunol 2004;173:4207–4217.

36. Puri A, Saxena R, Saxena RP, Saxena KC, Srivastava V, Tandon JS. Immunostimulant agents from Andrographis paniculata. J Nat Prod 1993;56:995–999.

37. Choudhury BR, Haque SJ, Poddar MK. In vivo and in vitro effects of kalmegh (Andrographis paniculata) extract and andrographolide on hepatic microsomal drug metabolizing enzymes. Planta Med 1987;53:135–140.

38. Matsuda T, Kuroyanagi M, Sugiyama S, Umehara K, Ueno A, Nishi K. Cell differentiation-inducing diterpenes from Andrographis paniculata Nees. Chem Pharm Bull (Tokyo) 1994;42:1216–1225.

39. Manikam SD, Stanslas J. Andrographolide inhibits growth of acute promyelocytic leukaemia cells by inducing retinoic acid receptor-independent cell differentiation and apoptosis. J Pharm Pharmacol 2009;61:69–78.

40. Han C, Barrios FJ, Riofski MV, Colby DA. Semisynthetic derivatives of sesquiterpene lactones by palladium-catalyzed arylation of the alpha-methylene-gamma-lactone substructure. J Org Chem 2009;74:7176–7179.

41. Dalton WS, Hazlehurst L, Shain K, Landowski T, Alsina M. Targeting the bone marrow microenvironment in hematologic malignancies. Semin Hematol 2004;41(Suppl. 4):1–5.

42. Tancred TM, Belch AR, Reiman T, Pilarski LM, Kirshner J. Altered expression of fibronectin and collagens I and IV in multiple myeloma and monoclonal gammopathy of undetermined significance. J Histochem Cytochem 2009;57:239–247.

43. Kwok BH, Koh B, Ndubuisi MI, Elofsson M, Crews CM. The anti-inflammatory natural product parthenolide from the medicinal herb feverfew directly binds to and inhibits IkappaB kinase. Chem Biol 2001;8:759–766.

44. Matsui W, Huff CA, Wang Q, Malehorn MT, Barber J, Tanhehco Y, Smith BD, Civin CI, Jones RJ. Characterization of clonogenic multiple myeloma cells. Blood 2004;103:2332–2336.

45. Matsui W, Wang Q, Barber JP, et al. Clonogenic multiple myeloma progenitors, stem cell properties, and drug resistance. Cancer Res 2008;68:190–197.

46. Cheung WC, Van Ness B. Distinct IL-6 signal transduction leads to growth arrest and death in B cells or growth promotion and cell survival in myeloma cells. Leukemia 2002;16:1182–1188.

47. Gupta PB, Onder TT, Jiang G, et al. Identification of selective inhibitors of cancer stem cells by high-throughput screening. Cell 2009;138:645–659.

48. Hazlehurst LA, Dalton WS. Mechanisms associated with cell adhesion mediated drug resistance (CAM-DR) in hematopoietic malignancies. Cancer Metastasis Rev 2001;20:43–50.

49. Nefedova Y, Landowski TH, Dalton WS. Bone marrow stromal-derived soluble factors and direct cell contact contribute to de novo drug resistance of myeloma cells by distinct mechanisms. Leukemia 2003;17:1175–1182.

50. Perez LE, Parquet N, Shain K, et al. Bone marrow stroma confers resistance to Apo2 ligand/TRAIL in multiple myeloma in part by regulating c-FLIP. J Immunol 2008;180:1545–1555.